

## COMMUNICATION

# Adding a Lysine Mimic in the Design of Potent Inhibitors of Histone Lysine Methyltransferases

Yanqi Chang<sup>1</sup>†, Thota Ganesh<sup>2</sup>†, John R. Horton<sup>1</sup>, Astrid Spannhoff<sup>3</sup>, Jin Liu<sup>2</sup>, Aiming Sun<sup>2</sup>, Xing Zhang<sup>1</sup>, Mark T. Bedford<sup>3</sup>, Yoichi Shinkai<sup>4</sup>, James P. Snyder<sup>2\*</sup> and Xiaodong Cheng<sup>1\*</sup>

<sup>1</sup>Department of Biochemistry, Emory University, Atlanta, GA 30322, USA

<sup>2</sup>Department of Chemistry, Emory University, Atlanta, GA 30322, USA

<sup>3</sup>Department of Carcinogenesis, University of Texas, M.D. Anderson Cancer Center, 1808 Park Road 1C, Smithville, TX 78957, USA

<sup>4</sup>Experimental Research Center for Infectious Diseases, Institute for Virus Research, Kyoto University, 53 Shogoin, Kawara-cho, Sakyo-ku, Kyoto 606-8507, Japan

Received 29 March 2010;  
received in revised form  
22 April 2010;  
accepted 23 April 2010  
Available online  
29 April 2010

Dynamic histone lysine methylation involves the activities of modifying enzymes (writers), enzymes removing modifications (erasers), and readers of the histone code. One common feature of these activities is the recognition of lysines in methylated and unmethylated states, whether they are substrates, reaction products, or binding partners. We applied the concept of adding a lysine mimic to an established inhibitor (BIX-01294) of histone H3 lysine 9 methyltransferases G9a and G9a-like protein by including a 5-aminopentyloxy moiety, which is inserted into the target lysine-binding channel and becomes methylated by G9a-like protein, albeit slowly. The compound enhances its potency *in vitro* and reduces cell toxicity *in vivo*. We suggest that adding a lysine or methyl-lysine mimic should be considered in the design of small-molecule inhibitors for other methyl-lysine writers, erasers, and readers.

© 2010 Elsevier Ltd. All rights reserved.

Edited by J. Karn

Keywords: epigenetics; histone lysine methylation; enzymatic inhibition; lysine mimics

Chromatin, rather than being a passive platform to store genetic information, can regulate transcriptional processes based on modifications of both DNA and histones. Histones are subject to an array of posttranslational modifications, including methylation of lysines. These marks are generated by a host

of histone methyltransferases, removed by histone demethylases, and recognized by reader domains in the methylated and unmodified states. Importantly, such enzymes are novel targets for therapeutics.<sup>1,2</sup>

BIX-01294 (a diazepin-quinazolin-amine derivative) inhibits activities of G9a and G9a-like protein (GLP) lysine methyltransferase (IC<sub>50</sub> in low micromolar range)<sup>3–5</sup> and reduces the methylation levels of histone H3 lysine 9 (H3K9) at several G9a target genes.<sup>3,6,7</sup> BIX-01294 (BIX) consists of a central quinazoline ring linked to a seven-membered diazepane ring and a benzylated six-membered piperidine ring (Fig. 1a). Structural comparison of GLP of BIX-bound with that of substrate peptide-bound<sup>9</sup> suggested that

\*Corresponding authors. E-mail addresses: jsnyder@emory.edu; xcheng@emory.edu.

† Y.C. and T.G. contributed equally to this work.  
Abbreviations used: GLP, G9a-like protein; H3K9, histone H3 lysine 9; AdoHcy, S-adenosyl-L-homocysteine; DMSO, dimethyl sulfoxide; AdoMet, S-adenosyl-L-methionine; PDB, Protein Data Bank.

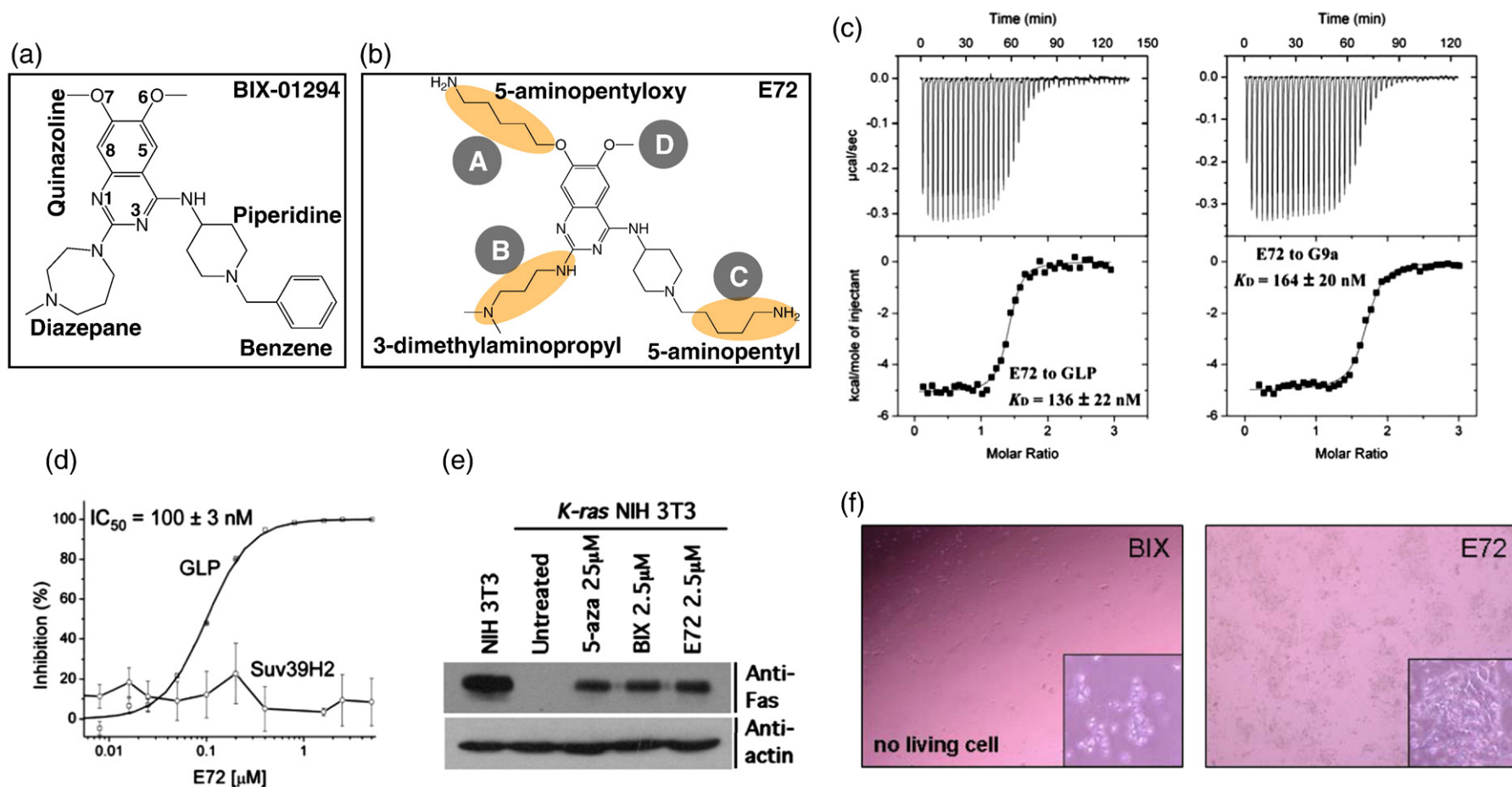


**Fig. 1.** Chemical structures for (a) BIX-01294 and (b) E72, highlighted with changes. (c) The binding ( $K_d$  values) of E72 compound to GLP (left panel) and G9a (right panel) is measured by isothermal titration calorimetry with a VP-ITC instrument (MicroCal) at 25 °C. The titrations were conducted in buffer containing 20 mM Tris, pH 8.0, 150 mM NaCl, 1.3–1.45% DMSO, and 50 μM AdoMet. The sample chamber and syringe were filled with 20–30 μM GLP (or 21 μM G9a) and 260–350 μM (or 286 μM) compound, respectively. The data were processed using Origin 7.0 software. (d) The inhibition ( $IC_{50}$  values) of E72 against GLP or Suv39H2 is plotted against various concentrations of compound, under the conditions of 0.075 μM GLP or Suv39H2, 10 μM H3 peptide (residues 1–15), 100 μM AdoMet in the buffer of 20 mM Tris, pH 8.5, 5 mM DTT, and 2% DMSO. The reaction mixture was incubated for 5 min (GLP) or 15 min (Suv39H2) at 30 °C and subjected to mass-spectrometry-based inhibition assay as previously described.<sup>4</sup> (e) Ras-mediated epigenetic silencing of Fas is derepressed with E72, BIX, and 5-aza treatments, as previously described.<sup>4</sup> (f) Mouse embryonic stem cells (TT2)<sup>8</sup> were treated for 24 h with each compound at 10 μM concentration: BIX-01294 (left) and E72 (right) (see also [Supplementary Table 1](#) and [Fig. 3b](#)).

BIX resembles the bound conformation of histone H3 Lys4 to Arg8, residues N-terminal to the target lysine, but leaves the target lysine-binding channel unoccupied.<sup>4</sup> Herein we report the use of the co-crystal structure of the GLP–BIX complex<sup>4</sup> and molecular modeling to guide the design, synthesis, and validation of new BIX derivatives with moieties mimicking lysine and methyl-lysine.

### Adding lysine and methyl-lysine mimics

We replaced the O7-methoxy group with a 5-aminopentyloxy substituent at site A (Fig. 1b). The length of the aliphatic chain and the presence of a terminal amino group for the 5-aminopentyloxy moiety were expected to extend into the active site of GLP and mimic the side chain of a substrate lysine. In addition, we replaced the diazepane ring and the benzyl with a 3-dimethylaminopropyl and a 5-aminopentyl group at sites B and C, respectively. These modifications generated compound E72 (Fig. 1b). The 3-dimethylaminopropyl unit contains a three-carbon aliphatic chain and a di-methylated amino moiety that was expected to form a favorable electrostatic interaction with Asp1131 of GLP.<sup>4</sup> The benzyl functionality is not well defined in the structure of the GLP–BIX complex,<sup>4</sup> because the branched benzene moiety has little direct contact with the enzyme. Taken together, these modifications resulted in the dissociation constant ( $K_d$ ) of approximately 136 nM (Fig. 1c, left panel) and half-maximal inhibitory concentration ( $IC_{50}$ ) of 100 nM (Fig. 1d) for E72 against GLP under linear reaction conditions by mass-spectrometry-based inhibition assay.<sup>4</sup> The cumulative effect of these changes in E72 is to decrease  $IC_{50}$  by a factor of approximately 7 in comparison to that of BIX measured by the same assay.<sup>4</sup>

E72 retains the binding affinity towards G9a (Fig. 1c, right panel), selectivity over the related H3K9 methyltransferase Suv39H2 (Fig. 1d; Supplementary Fig. S1), and the ability to reactivate K-ras-mediated epigenetic silencing of the proapoptotic Fas gene in NIH 3T3 cell (Fig. 1e). More importantly, E72 has much reduced cell cytotoxicity (Fig. 1f). In all three cell types treated (Supplementary Table 1), very little toxicity was observed for E72 at 10  $\mu$ M concentration, while BIX killed almost all cells at 10  $\mu$ M and approximately 50% at 1  $\mu$ M.

### Structures of GLP bound with E72

We solved the ternary structure of GLP in complex with E72, in the presence of S-adenosyl-L-homocysteine (AdoHcy) at a resolution of 2.19 Å (Supplementary Table 2). The E72 compound was co-crystallized with GLP–AdoHcy in the space group  $P2_1$ , at 16 °C by mixing equal volumes of protein (at 18–20 mg/ml) with solution containing 2 mM compound in 0.1 M Hepes, pH 7.5, 14% polyethylene glycol 4000, 9% isopropanol, and 12% dimethyl sulfoxide (DMSO). There are four molecules per crystallographic asymmetric unit. The structures of the protein component are highly similar (with root-

mean-square deviation of  $\sim 0.2$ – $0.6$  Å of 1020 pairs of main-chain atoms between the monomers).

E72 is bound to the acidic surface of the histone H3 peptide-binding groove (Fig. 2a), surrounded by many acidic residues including four aspartates, Asp1131, Asp1135, Asp1140, and Asp1145. Two of them, Asp1140 and Asp1145, maintain the same sets of hydrogen-bonding interactions described previously for BIX<sup>4</sup> with the linker NH group between the quinazoline and piperidine rings and the N1 ring nitrogen atom of the quinazoline, respectively (Fig. 2b). Additionally, Asp1131 forms a salt bridge with the dimethylamino group as expected (Fig. 2a and b). The three-carbon aliphatic chain may be optimal for the formation of this charge–charge interaction, as reducing or increasing the chain length by one carbon resulted in less inhibition under a single inhibitor concentration tested (Supplementary Fig. S2).

In E72, the O7 5-aminopentyloxy moiety at site A is extended into the target lysine-binding channel (Fig. 2c). Aromatic residues, Phe1144, Phe1209, and Tyr1211, wrap around the aliphatic chain (Fig. 2c), while the terminal amino group forms a hydrogen bond with the main-chain carbonyl oxygen of Ser1141 (Fig. 2b). The terminal amino group is only approximately 4.2 Å from the AdoHcy sulfur atom (Fig. 2b), where the transferable methyl group would be attached to S-adenosyl-L-methionine (AdoMet). In comparison, in the ternary structure of GLP in complex with AdoHcy and histone H3 peptide containing monomethylated lysine 9 (H3K9me1),<sup>9</sup> the distances between the AdoHcy sulfur atom and the methyl group or the target nitrogen are approximately 3.3 Å (S..CH<sub>3</sub>) or 4.7 Å (S..N) (Fig. 2d), respectively. Superimposition of the E72 complex and the H3K9me1 peptide complex structures reveals that the position of the 5-aminopentyloxy moiety coincides with that of lysine 9 of histone H3 (Fig. 2e). This observation suggested that E72 might potentially be a substrate for methylation by GLP. Indeed, after long incubations (overnight) with a nearly equimolar ratio of enzyme to compound, E72 is mono- or even di- and tri-methylated by GLP (Fig. 2f).

The 5-aminopentyl moiety attached to the piperidine ring at site C sits in an acidic surface groove that is formed by Asp1135 and Val1136 on one side, Asp1140 and Asp1138 on the other, and the main-chain atoms of Arg1137 on the floor (Fig. 2a). The terminal amino group points out into the solvent and might involve in an electrostatic association between the C-NH<sub>3</sub><sup>+</sup> of the ligand and the backbone C=O of Val1136, because the two bonds are parallel and separated by approximately 3.9 Å. In the structures of GLP in complex with BIX<sup>4</sup> as well as E67 (the compounds retain the benzyl moiety on the piperidine; Fig. 3a), the density for the benzyl moiety is not well defined (Supplementary Fig. S3a). This result suggests that, with respect to the 5-aminopentyl moiety at site C, the enhanced potency of E72 by approximately a factor of 3 (comparing the  $IC_{50}$  value to that of E67; Fig. 3a) is likely due to van der Waals contacts between the groove and the aliphatic chain of this moiety.

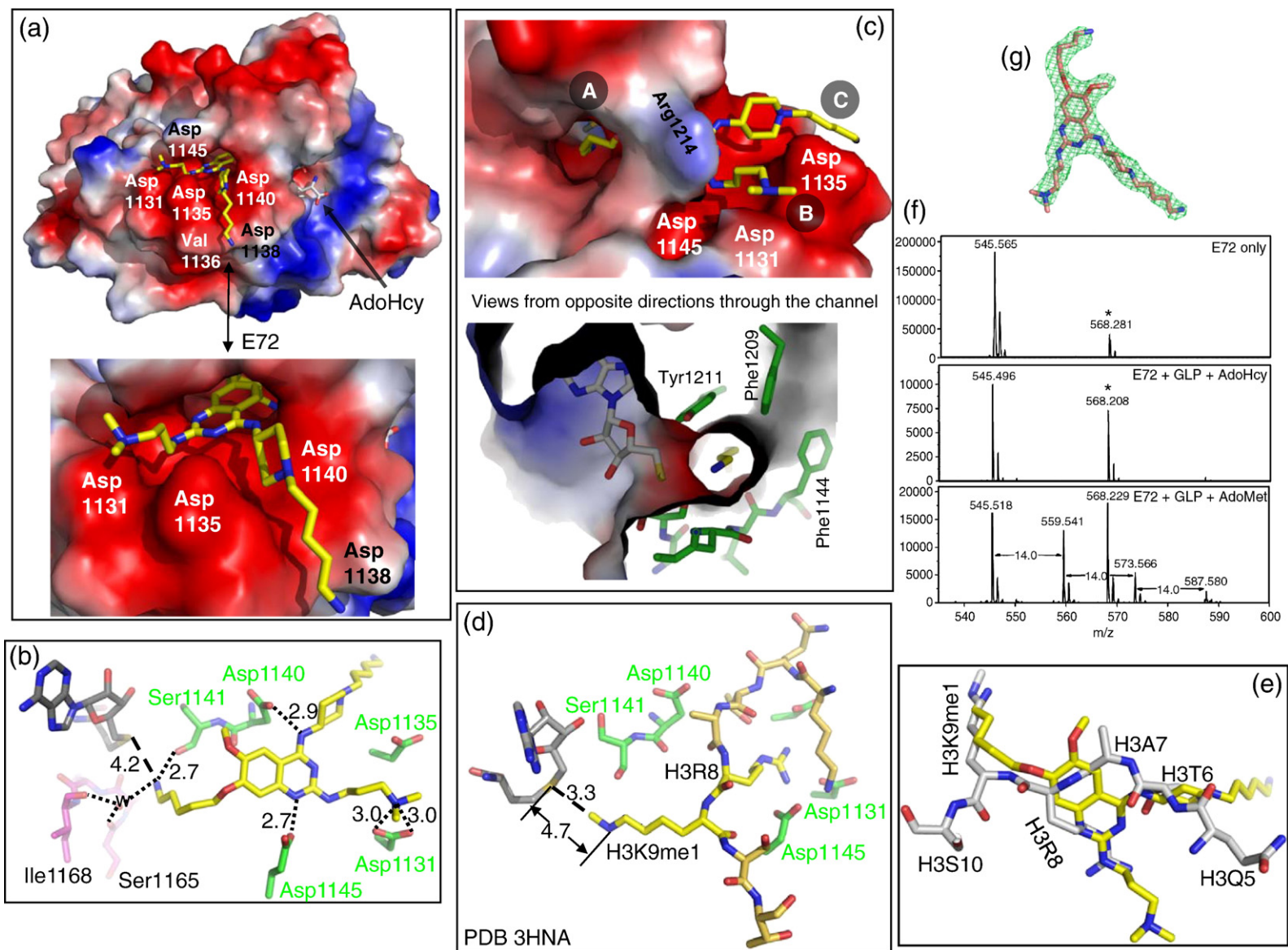
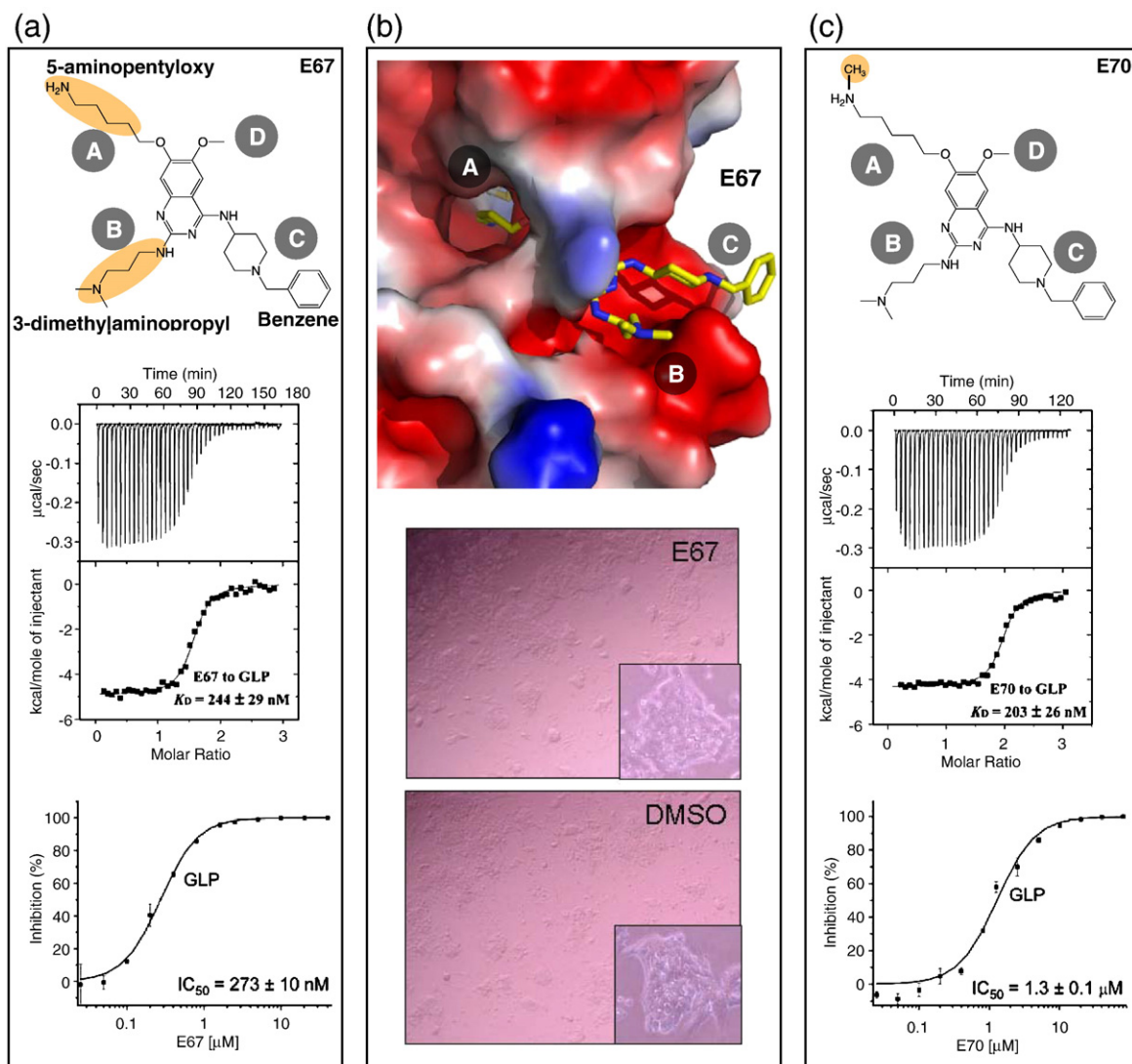


Fig. 2 (legend on next page)



**Fig. 3.** Comparison of compound E67 and E70 (mono-methylated analog of E67). (a) Top panel shows the chemical structure of E67; the middle and bottom panels show the measurements of  $K_d$  and  $IC_{50}$  against GLP. (b) Top panel shows the structure of the GLP-AdoHcy-E67 complex (Supplementary Table 2). The 5-aminopentyloxy moiety occupies the target lysine-binding channel. Bottom panels show the reduced cell toxicity of E67. Mouse embryonic stem cells (TT2) were treated for 24 h with E67 compound at 10 µM concentration. The experiments were performed together with BIX-01294 and E72 (Fig. 1f) and control DMSO (see Supplementary Table 1). (c) Top panel shows the chemical structure of E70; the middle and bottom panels show the measurements of  $K_d$  and  $IC_{50}$  against GLP.

### Compound E67 and its mono-methylated analog (E70)

The 5-aminopentyloxy moiety at site A that is inserted into the target lysine-binding channel in

both E72 (Fig. 2) and E67 (Fig. 3b) appears to be optimal for inhibition because compounds containing one fewer methylene unit are weaker inhibitors of the enzyme (4C compounds in Supplementary Fig. S4). Interestingly, the compounds containing

**Fig. 2.** Structure of GLP-E72-AdoHcy complex. (a) Surface representation of the GLP catalytic domain with AdoHcy and E72 bound in two distinctive pockets. The surface charge at neutral pH is displayed as red for negative, blue for positive, and white for neutral. (b) Network of hydrogen bonds centered on E72. (c) The 5-aminopentyloxy moiety occupies the target lysine-binding channel; views from opposite directions. (d) The structure of GLP-AdoHcy-histone H3 peptide containing H3K9me1 (PDB ID: 3HNA).<sup>9</sup> (e) Superimposition of histone H3 peptide (taken from PDB ID: 3HNA) and E72 (yellow). (f) E72 is methylated by GLP under the reaction conditions of 1.5 µM GLP, 1.6 µM E72, 100 µM AdoMet in the buffer of 20 mM Tris, pH 8.5, 5 mM DTT, and 2% DMSO. The mixture was incubated for 3 h at 30 °C and then overnight (~16 h) at room temperature (~21 °C). The mass peak at 568 Da (indicated by an asterisk) is from the matrix used in the mass spectra measurement (Supplementary Fig. S3b). (g) Omit electron density,  $F_o - F_c$  (green mesh), contoured at 4  $\sigma$  above the mean, is shown for E72.

one additional methylene (6C compounds) showed inhibition comparable to that of compounds with five methylene units (5C in [Supplementary Fig. S4](#)). This is probably because the length of the 6C aliphatic chain mimics the methylated 5-aminopentyl group. The mono-methylated E67 (compound E70) has a  $K_d$  value similar to that of the unmethylated form, but with reduced inhibitory effect by a factor of approximately 4 ([Fig. 3c](#)). Perhaps the E70–GLP complex represents a methylated product, resulting in a faster off rate of the ligand. Recently, Liu *et al.* synthesized a BIX analog (UNC0224) with a 3-(dimethylamino)propoxy moiety replacing the O7-methoxy group at site A.<sup>5</sup> While the central quinoxaline ring overlaps well with that of E72 and E67, the 3-(dimethylamino)propoxy side chain is two carbons too short to mimic a di-methylated lysine side chain in the active sites of G9a and GLP ([Supplementary Fig. S5](#) and [Supplementary Table 3](#)).

## Discussion

By including a moiety to mimic the lysine side chain at site A, we discovered that such modification can result in more effective inhibition of GLP (a H3K9 methyl writer) via a slow methylation reaction. The observations provide avenues for designing small-molecule inhibitors for other methyl-lysine writers, erasers, and readers by including a lysine or methyl-lysine mimic. For example, the 3-dimethylaminopropyl unit at site B containing a di-methylated amino group could be targeted by a di-methyl-lysine-specific Jumonji demethylase. The 5-aminopentyl group at site C might be targeted by a different SET domain protein. The modification of the O6 methoxy at site D, which interferes with the G9a/GLP–ligand interaction (data not shown), might provide an anchor for binding with other SET- or Jumonji-domain-containing proteins. Once the side-chain mimic at a specific branch is identified for a particular target, lysine or methyl-lysine mimics at other sites can conceivably be eliminated or replaced to improve the selectivity, and the length of the aliphatic chain can be optimized to improve potency. In conclusion, iterative cycles of crystallography, synthesis, and bioassay will aid successful design of epigenetic inhibitors of histone lysine methyltransferases as well as provide knowledge for future therapeutics that might be directly applicable to patients who are receiving epigenetic-based therapies (5-aza-2'-deoxycytidine and histone deacetylase inhibitors).<sup>10</sup>

Interestingly, the  $K_d$  and  $IC_{50}$  values for compounds E67 (244 nM and 273 nM) and E72 (136 nM and 100 nM) are approximately the same, whereas the  $K_d$  values for compounds BIX (97 nM and 647 nM) and E11 (154 nM and 778 nM) ([Supplementary Fig. S2](#)) are much lower than that of the corresponding  $IC_{50}$  value ([Supplementary Table 3](#)). It was somewhat puzzling that E72 and E67 compounds have lower  $IC_{50}$  than BIX and E11 yet have similar or even higher  $K_d$  for GLP. This may be

explained by the different modes of binding of these two groups of inhibitors. BIX and E11 occupy only part of the substrate peptide groove of GLP while leaving the target lysine channel open, so that they could be competed away by the substrate peptides relatively easily (indicated by the higher  $IC_{50}$  value than  $K_d$ ). E72 and E67, however, not only occupy the surface of the peptide-binding groove but also intercalate into the lysine-binding channel so that each binding event leads to effective inhibition; that is, the  $K_d$  and  $IC_{50}$  values are in agreement.

## Molecular modeling

Many of the compounds prepared as background to this study were modeled by Glide docking of candidate structures into the GLP–BIX complex<sup>4</sup> followed by MM–GBSA rescoring. Since this procedure essentially provides superposition of BIX-01294 with the crystal structure, it was used throughout in the search for improved BIX analogs. We illustrate the prediction for compound E72 in [Supplementary Fig. S6](#). The GLP–BIX–AdoHcy complex X-ray structure [Protein Data Bank (PDB) ID: 3FPD] was relieved of the BIX ligand in Maestro 8.5.111 (Schrodinger<sup>‡</sup>) and subjected to precision flexible Glide docking<sup>11,12</sup> with each new ligand structure. Based on the Glide scoring function, 20 poses were saved and then rescored with MM–GBSA.<sup>13,14</sup> The resulting pose with the best-calculated binding affinity was selected as the optimal docking solution.

## Chemical synthesis

Compound **1** was prepared as previously described<sup>15</sup> and reduced with tin (II) chloride<sup>16</sup> ([Supplementary Fig. S7](#)). The intermediate anthranilic acid was subsequently combined with sodium cyanate, followed by  $POCl_3$ , to provide **2**.<sup>17,18</sup> Treatment of the latter with 4-amino-1-benzylpiperidine in the presence of triethylamine delivered **3**, which was hydrogenated to produce a 3:1 mixture of **4** and **5**. These building blocks were individually coupled with 5-bromopentenenitrile in the presence of potassium carbonate to produce **6** and **8**. Finally, these compounds were treated with *N,N*-dimethylaminopropylamine at high temperature to provide precursors that were reduced by lithium aluminum hydride to furnish **7** (E67) and **9** (E72). Liquid chromatography–mass spectrometry and NMR were used to analyze the homogeneity of the synthesized compounds ([Supplementary Fig. S8](#)).

## PDB accession numbers

The coordinates and structure factor for human GLP catalytic domain bound with E72, E67, and E11, respectively, and AdoHcy have been deposited with accession numbers 3MO5, 3MO2, and 3MO0.

<sup>‡</sup> <http://www.schrodinger.com/>

## Acknowledgements

We thank Paul R. Thompson and Corey Causey for critical comments, Anup K. Upadhyay for discussion and advice on use of mass spectrometry, and Dennis Liotta for encouragement. The Biochemistry Department of Emory University School of Medicine supported the use of SER-CAT beamlines and mass spectrometry. This work was supported by grants R01GM068680 (to X.C. and X.Z.), R56DK082678 (to X.C. and Y.S.), and U54HG003918 from the National Institutes of Health and the Welch Foundation Grant G-1495 (to M.T.B.). X.C. is a Georgia Research Alliance Eminent Scholar.

**Author Contributions.** Y.C. performed SET-domain enzyme purifications, mass spectrometry-based inhibition assays, ITC measurements, crystallization, and participated in X-ray data collection; T.G. performed compound design, chemical synthesis, and wrote the method of chemical synthesis; J.R.H. collected X-ray data, determined structures and performed structural refinements; A.S. and M.T.B. performed Fas reactivation; J.L. performed Glide docking and contributed to compound design; A.S. assisted with compound design; X.Z. developed and optimized mass spectrometry-based assay; Y.S. performed cell toxicity assay; J.P.S. coordinated synthesis and modeling activities, contributed to compound design, and wrote method of molecular modeling and legend of supplementary figure S6; X.C. organized and designed the scope of the study, participated in designing compounds with T.G., and wrote the manuscript; all were involved in analyzing data and helped in revising the manuscript.

## Supplementary Data

Supplementary data associated with this article can be found, in the online version, at [doi:10.1016/j.jmb.2010.04.048](https://doi.org/10.1016/j.jmb.2010.04.048)

## References

1. Cole, P. A. (2008). Chemical probes for histone-modifying enzymes. *Nat. Chem. Biol.* **4**, 590–597.
2. Copeland, R. A., Solomon, M. E. & Richon, V. M. (2009). Protein methyltransferases as a target class for drug discovery. *Nat. Rev., Drug Discov.* **8**, 724–732.
3. Kubicek, S., O'Sullivan, R. J., August, E. M., Hickey, E. R., Zhang, Q., Teodoro, M. L. *et al.* (2007). Reversal of H3K9me2 by a small-molecule inhibitor for the G9a histone methyltransferase. *Mol. Cell*, **25**, 473–481.
4. Chang, Y., Zhang, X., Horton, J. R., Upadhyay, A. K., Spannhoff, A., Liu, J. *et al.* (2009). Structural basis for G9a-like protein lysine methyltransferase inhibition by BIX-01294. *Nat. Struct. Mol. Biol.* **16**, 312–317.
5. Liu, F., Chen, X., Allali-Hassani, A., Quinn, A. M., Wasney, G. A., Dong, A. *et al.* (2009). Discovery of a 2,4-diamino-7-aminoalkoxyquinazoline as a potent and selective inhibitor of histone lysine methyltransferase G9a. *J. Med. Chem.* **52**, 7950–7953.
6. Trojer, P., Zhang, J., Yonezawa, M., Schmidt, A., Zheng, H., Jenuwein, T. & Reinberg, D. (2009). Dynamic histone H1 isotype 4 methylation and demethylation by histone lysine methyltransferase G9a/KMT1C and the jumoni domain-containing JMJD2/KDM4 proteins. *J. Biol. Chem.* **284**, 8395–8405.
7. Maze, I., Covington, H. E., III, Dietz, D. M., LaPlant, Q., Renthal, W., Russo, S. J. *et al.* (2010). Essential role of the histone methyltransferase G9a in cocaine-induced plasticity. *Science*, **327**, 213–216.
8. Yagi, T., Tokunaga, T., Furuta, Y., Nada, S., Yoshida, M., Tsukada, T. *et al.* (1993). A novel ES cell line, TT2, with high germline-differentiating potency. *Anal. Biochem.* **214**, 70–76.
9. Wu, H., Min, J., Lunin, V. V., Antoshenko, T., Dombrovski, L., Zeng, H. *et al.* (2010). Structural biology of human H3K9 methyltransferases. *PLoS ONE*, **5**, e8570.
10. Karberg, S. (2009). Switching on epigenetic therapy. *Cell*, **139**, 1029–1031.
11. Friesner, R. A., Banks, J. L., Murphy, R. B., Halgren, T. A., Klicic, J. J., Mainz, D. T. *et al.* (2004). Glide: a new approach for rapid, accurate docking and scoring. 1. Method and assessment of docking accuracy. *J. Med. Chem.* **47**, 1739–1749.
12. Halgren, T. A., Murphy, R. B., Friesner, R. A., Beard, H. S., Frye, L. L., Pollard, W. T. & Banks, J. L. (2004). Glide: a new approach for rapid, accurate docking and scoring. 2. Enrichment factors in database screening. *J. Med. Chem.* **47**, 1750–1759.
13. Guimaraes, C. R. & Cardozo, M. (2008). MM-GB/SA rescoring of docking poses in structure-based lead optimization. *J. Chem. Inf. Model.* **48**, 958–970.
14. Lyne, P. D., Lamb, M. L. & Saeh, J. C. (2006). Accurate prediction of the relative potencies of members of a series of kinase inhibitors using molecular docking and MM-GBSA scoring. *J. Med. Chem.* **49**, 4805–4808.
15. Thurston, D. E., Murty, V. S., Langley, D. R. & Jones, G. B. (1990). O-Debenzylation of a pyrrolo [2,1-c][1,4]benzodiazepine in the presence of a carbinolamine functionality: synthesis of DC-81. *Synthesis*, **1**, 81–84.
16. Hu, W. P., Wang, J. J., Lin, F. L., Lin, Y. C., Lin, S. R. & Hsu, M. H. (2001). An efficient synthesis of pyrrolo [2,1-c][1,4]benzodiazepine. Synthesis of the antibiotic DC-81. *J. Org. Chem.* **66**, 2881–2883.
17. Andrus, M. B., Mettath, S. N. & Song, C. (2002). A modified synthesis of iodoazidoaryl prazosin. *J. Org. Chem.* **67**, 8284–8286.
18. Smits, R. A., de Esch, I. J., Zuiderveld, O. P., Broeker, J., Sansuk, K., Guaita, E. *et al.* (2008). Discovery of quinazolines as histamine H4 receptor inverse agonists using a scaffold hopping approach. *J. Med. Chem.* **51**, 7855–7865.